Near-Field Cosmology with Dwarf Elliptical Galaxies
Proceedings IAU Colloquium No. 198, 2005
H. Jerjen and B. Binggeli, eds.

doi:10.1017/S1743921305003741

3D Simulations of the ISM pollution by SNII and SNI in dwarf spheroidal galaxies

Andrea Marcolini[1], Fabrizio Brighenti[1] and Annibale D'Ercole[2]

[1] Dipartimento di Astronomia, Università di Bologna, via Ranzani 1, 40127 Bologna, Italy
[2] Osservatorio Astronomico di Bologna, via Ranzani 1, 40127 Bologna, Italy
email: andrea.marcolini@bo.astro.it

Abstract. We present preliminary results of 3-D hydro simulations of the interstellar medium evolution in dwarf spheroidal galaxies undergoing star formation for the first time. The star formation is assumed to occur in a sequence of instantaneus bursts separated by quiescent periods. Different models are made changing the number and the intensity of the bursts in such a way that the final mass of the formed stars remains the same. We followed the enrichment of the ISM taking into account the contribution of both type Ia and II supernovae. The aim of our models is to find a star formation history compatible with the observed spread of stellar age and metallicity in such galaxies and to reproduce the observed mass-metallicity relation.

Keywords. methods: numerical – galaxies: dwarf – galaxies: ISM – ISM: evolution

1. Introduction

The nearby dwarf spheroidal (dSph) galaxies offer an unique opportunity to study the dynamical and chemical feedback of star formation on the ISM and the resulting stellar population. The color-magnitude diagrams of these galaxies have revealed an unexpectedly complex star formation history (SFH). Many of these galaxies have formed stars at an approximately constant rate for a long time, of the order of a few (2–4) Gyr (e.g. Dolphin 2002). The large metallicity spread within individual galaxies (Shetrone, Cote' & Sargent 2001) and evidence of Type Ia supernova (SN) enrichment also indicate a prolonged SFH. These observational facts are puzzling and difficult to explain. The energy released by the SNe during the SF episodes largely exceeds the ISM binding energy and yet the delicate ISM is not disrupted or removed from the galaxy. Surprisingly, the SNe (and SNIa) heated the ISM with very low efficiency and this put strong constraints on the SFH and on the nature of the SN feedback. We are currently calculating a series of 3D hydrodynamical simulations of starforming dSph galaxies in order to find a plausible SFH and SN feedback which consistently explains the general properties of the stellar population.

2. The model

We have built a one parameter galaxy family (the parameter being the stellar mass, $M_{\star}$) which agrees with many observed relation (Peterson & Caldwell 1993, Mateo 1998). Each galaxy has initially two components: a spherical quasi isothermal dark halo and an isothermal ($T = T_{\mathrm{virial}}$) ISM in hydrostatic equilibrium in the gravitational potential of the dark matter. The initial gas mass is $M_{\mathrm{ISM}} \sim 0.15 M_{\mathrm{dark}}$, a value in reasonable agreement with the cosmological one (Spergel *et al.* 2003).

Table 1. Galaxy parameters

Model	$M_{\rm dark}$ ($10^7\,M_\odot$)	$\rho_{0,\rm d}$ (g cm^{-3})	$R_{\rm c,d}$ (pc)	$R_{\rm t,d}$ (kpc)	$M_{\rm ISM}$ ($10^6\,M_\odot$)	$\rho_{0,\rm ISM}$ (g cm^{-3})	$T_{\rm ISM}$ (K)	$E_{\rm bind}$ (10^{51} erg)	$M/L_{\rm V}$
Dra I	2.2	6.5×10^{-24}	160	1.0	3.0	2.3×10^{-24}	2×10^3	11	80
Dra II	7.7	4.3×10^{-24}	300	1.2	11.0	0.4×10^{-24}	1×10^4	66	280

The meaning of the simbols is as follows: $M_{\rm dark}$, $\rho_{0,\rm d}$, $R_{\rm c,d}$ and $R_{\rm t,d}$ are the mass, the central density, the core radius and the truncation radius of the dark matter halo; $M_{\rm ISM}$, $\rho_{0,\rm ISM}$, $T_{\rm ISM}$ and $E_{\rm bind}$ are the mass, the central density, the initial temperature and the binding energy of the ISM, respectively; $M/L_{\rm V}$ is the total mass to light ratio of the galaxy in the V band.

Table 2. Stellar and star formation parameters

Model	$M_\star$ ($10^6\,M_\odot$)	$\rho_{0,\rm s}$ (g cm^{-3})	$R_{\rm eff,s}$ (pc)	$R_{\rm c,s}$ (pc)	$R_{\rm t,s}$ (pc)	$N_{\rm SNII}$	$N_{\rm SNII}/N_{\rm bur}$	$\Delta t_{\rm bur}$ (Myr)	$N_{\rm SNI}$
Dra-50	0.56	1.0×10^{-24}	210	130	630	5.6×10^3	112	60	254
Dra-30	0.56	1.0×10^{-24}	210	130	630	5.6×10^3	224	120	257
Dra-10	0.56	1.0×10^{-24}	210	130	630	5.6×10^3	560	300	266

Here $M_\star$, $\rho_{0,\rm s}$, $R_{\rm eff,s}$, $R_{\rm c,s}$ and $R_{\rm t,s}$ are the final mass, central density, effective radius, core radius and truncation radius of the stellar component, respectively; $N_{\rm SNII}$ is the total number of SNII; $N_{\rm SNII}/N_{\rm burst}$ is the number of SNII in each burst; $\Delta t_{\rm burst}$ is the time interval between two succesive bursts and $N_{\rm SNI}$ is the total number of SNI at the end of the simulation.

We assume that stars form in a sequence of $N_{\rm burst}$ instantaneous bursts, separated by quiescent periods, in such a way that after 3 Gyr (the end of our simulation) the stellar mass agrees with the initially chosen one ($M_\star$). Several $N_{\rm burst}$ have been considered (see table 2). For simplicity, the stellar mass (a small fraction of the dark halo mass) does not contribute to the gravitational potential. With a typical stellar mass to light ratio of $M_\star/L_V = 2$ the total mass to light ratio fall in the observed range (see below). The SNII explode at a constant rate for a period of 30 Myr (the lifetime of a 8 $M_\odot$ star, the less massive SNII progenitor) after the occurrence of each stellar burst. Type Ia supernovae in each burst start to explode after 30 Myr and the rate decreases in time after a quick initial rise (Matteucci & Recchi 2001). Both type of SNe are stochastically placed according a spatial distribution given by a modified King profile (see Table 2 for details).

Here we present preliminary results relative to two galactic models taylored on a galaxy similar to Draco. The two models differ in the dark matter (and gas) content as illustrated in Table 1. For each of these models we considered three different star formation histories as illustrated in Table 2.

We solve the usual hydrodynamical equations through a second order espicit hydro code developed by the Bologna Hydrodynamics group. The numerical grid consistes of 160^3 mesh point. The central 100^3 mesh points (covering the stellar volume) have an uniform spatial separation of 13 pc, while the outer ones are distributed logarithmically. Outflow conditions are imposed at every boundary. Each supernova event is simulated by adding 10^{51} erg of thermal energy to the gas within a region with radius of 2 zones. In order to prevent the SN gas to cool too quickly the same region is devoided of its ISM content.

3. Results

Model Dra-I, with $M_{\rm dark} = 2.2 \times 10^7\ M_\odot$ is rapidly ($t < 200$ Myr) devoided of gas after few bursts for any of the three star formation histories adopted. Therefore this

https://doi.org/10.1017/S1743921305003741 Published online by Cambridge University Press

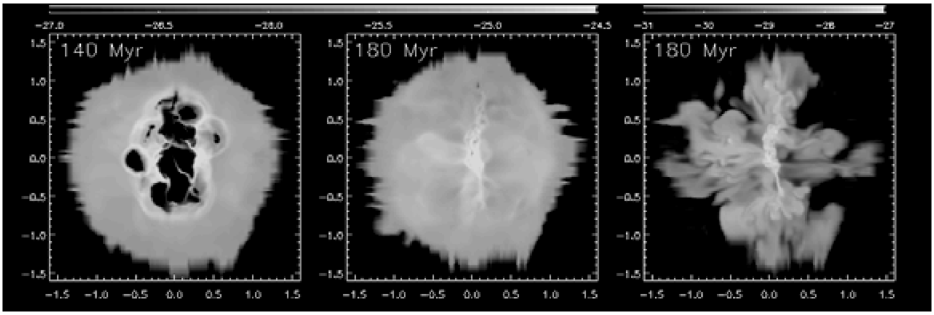

Figure 1. The two panel on the left show the density distribution of the ISM after 20 Myr and 60 Myr after the beginning of the third burst. The last panel illustrate the distribution of the metals ejected by the SNII at the same time of the central panel, immediately before the occurence of the new burst. Distances are given in kpc and density in g cm^{-3}.

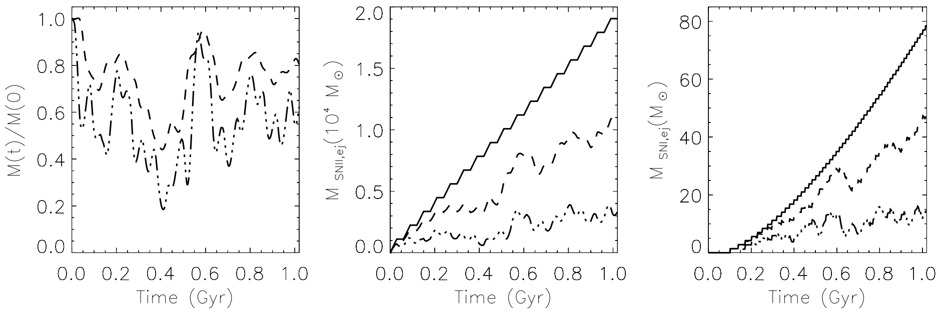

Figure 2. The first panel illustrates the evolution of the ISM mass within the dark matter and stellar volume normalized to the initial ISM mass. The second and third panel show the evolution of the SNII and SNI ejecta, respectively. Solid lines refer to the total ejecta mass produced by SNs, while dashed and point-dashed lines refer to the amount of mass in the dark halo and in the stellar region, respectively.

model is inconsistent with a prolonged SFH. Likely, larger dark matter halos are needed to retain the ISM for longer times. We thus describe below in some detail model Dra-II with $M_{\rm dark} = 7.7 \times 10^7$ $M_\odot$ (corrisponding to a total $M/L_V = 280$). Note that this model has a $M/L_V = 80$ within the stellar region. Preliminary results show that in this case supernovae are not able to remove the gas from the galaxy for the model DRA-50 and DRA-25.

We focus here on model DRA-50. When the SNIIs start to explode, they quickly collide and form a central very hot (up to $T = 10^8$ K) and tenuous medium. The cold and dense SNR shells interact each other forming filaments, and the mixture of the hot and cool gas is in a sort of turbulent equilibrium as long as SNII keep exploding (see Fig. 1). Then, during the quiescent time before the next starburst, radiative losses are no more balanced by SN energy input and the ISM cools down collapsing toward the centre. Figure 1 shows the ISM density distribution for this model at time $\Delta t = 20$ Myr (first panel) and $\Delta t = 60$ Myr (second panel) after the beginning of the third burst. As the secular evolution of the ISM is rather slow compared to the time interval between bursts, these shots are representative of the ISM evolution after any other starburst episode. The third panel in the figure shows the density of the SNII ejecta, at the same time of the central panel, immediately before the occurence of the next starburst. While most of the ejecta ($\sim$60% at 1 Gyr) is retained by the galactic potential well, only $1 - 4 \times 10^3$ $M_\odot$ ($\sim$15% at 1 Gyr) are present into the stellar volume at any time. This is apparent in

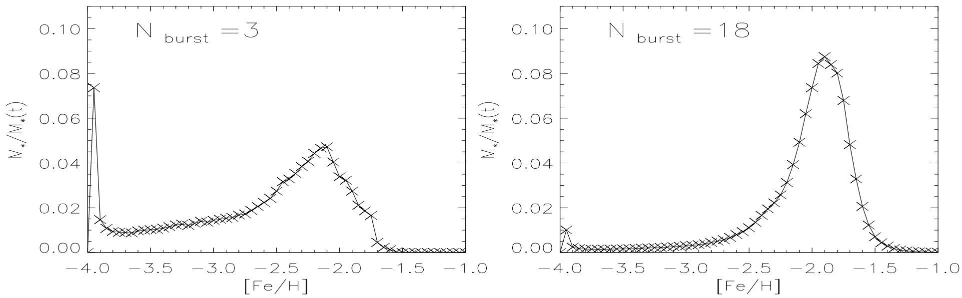

Figure 3. Metallicity distribution of the forming stars at two different times for the model DRA-50

Fig. 2 which shows the gas content evolution of the galaxy. The first panel illustrates the behavior of the ISM mass, while the central panel and the third panel illustrate the evolution of the content of the SNII and SNI ejecta, respectively.

In the first panel we see that almost all (∼80%) the gas remains bounded around the galaxy (at least for the first Gyr of star formation). The same is true for the SN ejecta. Note, however, the amount of metals into the stellar region grows very slowly, because each new burst "pushes" the present metals at larger radii.

In Fig. 3 we plot the mass of the forming stars versus their iron metallicity. This is obtained calculating the metallicity of the ISM immediately before each burst, and assuming that the density of the forming stars is proportional to the stellar King profile. As it is apparent, after few bursts, the stars tend to distribute in metallicity around [Fe/H] = −1.9 with a spread of 1 dex. Both the mean value and the spread are consistent with the observations (e.g. Aparicio, Carrera & Martinez-Delgado 2001).

References

Aparicio A., Carrera R. & Martnez-Delgado D. 2001, *AJ* 122, 2524
Dolphin A.E. 2002, *MNRAS* 332, 91
Fragile P.C., Murray S.D., Anninos P. & Lin D.N. 2003, *ApJ* 590, 778
Mateo M. 1998, *ARA&A* 36, 435
Matteucci F. & Recchi S. 2001, *ApJ* 558, 351
Peterson, R.C. & Caldwell, N. 1993, *AJ* 105, 1411
Shetrone, M.D., Côté, P. & Sargent WS.L.W. 2001, *ApJ* 548, 592
Spergel D.N. *et al.* 2003, *ApJS* 148, 175

Discussion

Hensler: What is the process in your numerical scheme that accounts for transfer of metals from the hot SN gas to the cool star-forming gas phase? Is it only cooling?

Marcolini: Yes. However, beside the metal dependent cooling implemented in the code, the numerical diffusion contributes to mix the SN ejecta with the cold gas. Altough such a diffusion mimics phisical mechanisms such as thermal conduction and mixing layers, we can not reproduce them quantitatively.

Lin: Is the SNe energy lost via radiative cooling, or is it dispersed into the IGM?

Marcolini: Even if a small fraction can be dispersed into the IGM, the majority of the energy is radiated away in this model.

https://doi.org/10.1017/S1743921305003741 Published online by Cambridge University Press